

Distributed Sign Momentum with Local Steps for Training Transformers

Shuhua Yu^{1*}, Ding Zhou², Cong Xie², An Xu², Zhi Zhang², Xin Liu², Soumya Kar¹

¹Carnegie Mellon University ²ByteDance Inc.

{shuhuay, soumyak}@andrew.cmu.edu

{ding.zhou, cong.xie, an.xu, zhangzhi.joshua, liuxin.ai}@bytedance.com

November, 2024

Abstract

Pre-training Transformer models is resource-intensive, and recent studies have shown that sign momentum is an efficient technique for training large-scale deep learning models, particularly Transformers. However, its application in distributed training or federated learning remains underexplored. This paper investigates a novel communication-efficient distributed sign momentum method with local updates. Our proposed method allows for a broad class of base optimizers for local updates, and uses sign momentum in global updates, where momentum is generated from differences accumulated during local steps. We evaluate our method on the pre-training of various GPT-2 models, and the empirical results show significant improvement compared to other distributed methods with local updates. Furthermore, by approximating the sign operator with a randomized version that acts as a continuous analog in expectation, we present an $O(1/\sqrt{T})$ convergence for one instance of the proposed method for nonconvex smooth functions.

1 Introduction

In this paper, we tackle the distributed optimization problem across n workers:

$$\underset{\mathbf{x} \in \mathbb{R}^d}{\text{minimize}} f(\mathbf{x}) := \frac{1}{n} \sum_{i=1}^n \mathbb{E}_{\xi^{(i)} \sim \mathcal{D}_i} F_i(\mathbf{x}, \xi^{(i)}),$$

where F_i represents the supervised learning model, \mathbf{x} denotes the model parameters, and $\xi^{(i)}$ refers to the data samples drawn from data distribution \mathcal{D}_i on worker $i \in [n]$. The problem formulation (1) serves as a natural abstraction for distributed training (Lian et al., 2017) and federated learning (McMahan et al., 2017). A common approach to solving (1) involves workers first computing mini-batch gradients of F_i , followed by an all-reduce step to aggregate the local mini-batch gradients and obtain the global average. A global optimization step, such as Stochastic Gradient Descent (SGD) (Robbins and Monro, 1951), Momentum (Polyak, 1964), Nesterov’s Accelerated Gradient (NAG) (Nesterov, 1983), Adam (Kingma, 2014) and its weight decay variant AdamW (Loshchilov, 2017), or more recently Lion (Chen et al., 2024b), is then applied. This method is well suited for distributed learning scenarios where data is spread across multiple workers due to size or privacy constraints, and communication is relatively inexpensive.

*Work partially done during the internship at ByteDance Inc.

However, in distributed training across GPU clusters, synchronized communication during the all-reduce step can become a bottleneck due to stragglers (Dean et al., 2012) or slow inter-node and inter-cluster communication. Several approaches have been proposed to mitigate this communication overhead. Decentralized methods, such as gossiping SGD (Jin et al., 2016) and consensus-based distributed SGD (Jiang et al., 2017), use approximate mini-batch gradient averaging instead of exact averaging to reduce idle time. Local updating methods, like local SGD (Gorbunov et al., 2021b; Lin et al., 2020), local momentum (PR-SGD-Momentum) (Yu et al., 2019) and local Adam (Lu et al., 2023), reduce communication frequency to save on bandwidth. Additionally, some local updating methods further optimize performance by overlapping communication and computation (Sun et al., 2024; Wang et al., 2019), utilizing stale synchronized model parameters for local updates to reduce the waiting time for synchronizing the latest local models. All these approaches, although reduce communication and run faster, add perturbations to the optimization process. These perturbations can lead to decreased performance in terms of training and validation losses under the same amount of computation, especially under heterogeneous local data (Wang et al., 2020).

Several methods have been proposed to enhance the performance of local updating techniques. SCAFFOLD (Karimireddy et al., 2020) introduces a control variate that corrects the local SGD direction using global information, eliminating the dependency on local gradient dissimilarity in the convergence guarantees. One of the most relevant methods, BMUF (Chen and Huo, 2016), combines local updates with a global momentum step to accelerate distributed training, without the need for additional communication, such as transmitting the control variate in SCAFFOLD or the local momentum in PR-SGD-Momentum (Yu et al., 2019). SlowMo (Wang et al., 2019) extends BMUF by providing a general framework that operates on local base optimizers, such as local SGD and SGP (Assran et al., 2019), and periodically applies a global momentum step after running the local optimizer for several iterations.

Beyond local updating methods, momentum has long been recognized as a key technique for improving deep learning training, enhancing both optimization and generalization (Sutskever et al., 2013). More recently, Kunstner et al. (2023) suggest that sign momentum may be the key factor behind Adam’s significant advantage over SGD in training Transformers (Vaswani, 2017). Chen et al. (2024b) introduced the Lion (Evolved Sign Momentum) optimization method, discovered through program search, which outperforms the widely used Adam (Kingma, 2014) in various vision and autoregressive language modeling tasks. Furthermore, Kunstner et al. (2023), through experiments with different batch sizes, suggest that Adam’s significant performance advantage over SGD likely stems from its similarity to sign descent with momentum, particularly in Transformers used for language models.

Inspired by the effectiveness of the sign momentum method in training large neural networks, particularly Transformers, and the success of global momentum steps in local updating methods, a natural question is:

Can we extend the sign momentum method to distributed training of Transformers with local updates?

1.1 Contributions

In this work, we answer this question affirmatively by proposing a framework for distributed sign momentum with local updates, supported by both empirical evaluations and theoretical justifications. Our contributions are as follows:

- (a) We introduce a new framework for distributed sign momentum with local updates. This framework is versatile, allowing any off-the-shelf base optimizers for local updates, while using differences accumulated from these updates to adjust the momentum in the global sign momentum step. Details are provided in Algorithm 1.
- (b) We evaluate the performance of Algorithm 1 in pre-training GPT-2 models of various sizes, demonstrating consistent improvements over other local updating methods. In the special single worker case, Algorithm 1 and its non-signed variant can even outperform AdamW.

- (c) We provide a general theoretical analysis of the proposed framework by approximating the sign operator with a randomized continuous analog in expectation. When specializing the base optimizer as SGD, we obtain an $O(1/\sqrt{T})$ convergence where T is the total global steps.

1.2 Related work

Communication compression. In distributed optimization, there has been extensive research on compressing communication between workers to reduce overhead. This includes methods such as 1-bit sign SGD (Bernstein et al., 2018; Seide et al., 2014), gradient difference compression (Gorbunov et al., 2021a), compression with error-feedback (Karimireddy et al., 2019), and compression with error reset (Xie et al., 2020), among others. Although this work focuses on local updating methods without communication compression, several 1-bit compression (sign-based) methods, such as SIGNUM (Bernstein et al., 2019) and Major Vote signSGD (Sun et al., 2023), apply (random) sign operations to local momentum and use majority voting for local signs. In contrast, Algorithm 1 employs full-precision communication during the global synchronization step, with the sign taken after aggregation.

signSGD and its momentum variants. The convergence of signSGD and its momentum variants has been studied for nonconvex and smooth functions. For signSGD, defined as:

$$\mathbf{x}_{t+1} = \mathbf{x}_t - \eta_t \text{sign}(\nabla f(\mathbf{x}_t, \boldsymbol{\xi}_t)), \quad (1)$$

an $O(T^{-1/4})$ convergence rate has been established under an increasing batch size (Bernstein et al., 2018), or under unimodal and symmetric stochastic gradients (Bernstein et al., 2019). For signSGD with a momentum buffer \mathbf{m}_t , given by:

$$\begin{aligned} \mathbf{m}_{t+1} &= \beta \mathbf{m}_t + (1 - \beta) \nabla f(\mathbf{x}_t, \boldsymbol{\xi}_t), \\ \mathbf{x}_{t+1} &= \mathbf{x}_t - \eta_t \text{sign}(\mathbf{m}_{t+1}), \end{aligned} \quad (2)$$

its $O(1/T^{-1/4})$ convergence rate is guaranteed under a decreasing step size and increasing batch size, as shown by Bernstein et al. (2018). Sun et al. (2023) improve the previous results by showing the same convergence rate under a *constant* batch size independent of T . Additionally, Karimireddy et al. (2019) shows that signSGD with error-feedback, another momentum variant, also achieves an $O(T^{-1/4})$ convergence rate, albeit under a more stringent bounded stochastic gradient condition.

2 Distributed sign momentum

We introduce a general framework, outlined in Algorithm 1, that can incorporate any off-the-shelf base optimizer within the inner loop. Each worker $i \in [n]$ maintains a local model copy $\mathbf{x}_{t,k}^{(i)}$ for the outer iteration t and inner iteration k , denoted as (t, k) . Specifically, at t -th outer iteration, each worker $i \in [n]$ performs τ local model updates:

$$\mathbf{x}_{t,k+1}^{(i)} = \mathbf{x}_{t,k}^{(i)} - \gamma_t \mathbf{d}_{t,k}^{(i)}, \quad k = 0, \dots, \tau - 1, \quad (3)$$

where γ_t is the local learning rate (LR) and $\mathbf{d}_{t,k}^{(i)}$ is the update direction of local base optimizer. We allow for any base optimizers, such as SGD (with or without momentum), AdamW, and others. For example, if the base optimizer is mini-batch SGD, then

$$\mathbf{d}_{t,k}^{(i)} = \nabla F_i(\mathbf{x}_{t,k}^{(i)}, \boldsymbol{\xi}_{t,k}^{(i)}), \quad (4)$$

where $\boldsymbol{\xi}_{t,k}^{(i)}$ is a sample drawn from $\boldsymbol{\xi}^{(i)}$. As in Wang et al. (2019), base optimizers can also involve communication steps, such as SGP (Assran et al., 2019), and momentum steps. We denote the final update direction applied to worker i at iteration (t, k) as $\mathbf{d}_{t,k}^{(i)}$.

After τ local steps using the base optimizer, the workers communicate to perform a global sign momentum step. Two global buffers are maintained: the model buffer $\mathbf{x}_{t,0}$ and the momentum buffer \mathbf{m}_0 . All workers are assumed to be initialized with $\mathbf{x}_{0,0}$ and $\mathbf{m}_0 = \mathbf{0}$. First, an all-reduce operation is performed to compute the average of the local models, i.e., $\mathbf{x}_{t,\tau} = (1/n) \sum_{i=1}^n \mathbf{x}_{t,\tau}^{(i)}$. The momentum buffer is then used to execute the global sign momentum step (line 9), for some $\beta_1 \in [0, 1]$,

$$\mathbf{u}_{t+1} = \beta_1 \mathbf{m}_t + \frac{1 - \beta_1}{\gamma_t} (\mathbf{x}_{t,0} - \mathbf{x}_{t,\tau}), \quad (5)$$

$$\mathbf{x}_{t+1,0} = \mathbf{x}_{t,0} - \eta \gamma_t (\text{sign}(\mathbf{u}_{t+1}) + \lambda \mathbf{x}_{t,0}), \quad (6)$$

where η is the global learning rate and λ is the decoupled weight decay. Then, we perform the following global momentum update (line 8), for some $\beta_2 \in [0, 1]$,

$$\mathbf{m}_{t+1} = \beta_2 \mathbf{m}_t + \frac{1 - \beta_2}{\gamma_t} (\mathbf{x}_{t,0} - \mathbf{x}_{t,\tau}). \quad (7)$$

Note that (5)-(7) mimics the update rule of Lion (Chen et al., 2024a) (also described in in Section A in Appendix), by treating the differences accumulated from local updates as pseudo-stochastic gradients. In both (5) and (7), we scale $(\mathbf{x}_{t,0} - \mathbf{x}_{t,\tau})$ by $\frac{1}{\gamma_t}$ to make the momentum buffer independent of the learning rate γ_t , which can vary over time when using a learning rate schedule.

Algorithm instances. Instances of Algorithm 1 can be obtained by specifying the parameters $\eta, \gamma_t, \beta_1, \beta_2, \lambda$. For example, setting $\beta_1 = \beta_2 = \beta, \lambda = 0, \tau = 1$ recovers signSGD with momentum as described in (2). In particular, when $n = 1$, Algorithm 1 simplifies to a signed Lookahead optimizer (Zhang et al., 2019) with decoupled weight decay.

Algorithm 1 Distributed Sign Momentum

Require: Local update directions $\mathbf{d}_{t,k}^{(i)}$, local learning rate γ , global learning rate η , momentum coefficients β_1, β_2 .

- 1: Initialize $\mathbf{x}_{0,0}$, let $\mathbf{m}_0 = \mathbf{0}$.
 - 2: **for** $t = 0$ to $T - 1$ **do**
 - 3: **for** $i = 1$ to n in parallel **do**
 - 4: **for** $k = 0$ to $\tau - 1$ **do**
 - 5: $\mathbf{x}_{t,k+1}^{(i)} \leftarrow \mathbf{x}_{t,k}^{(i)} - \gamma_t \mathbf{d}_{t,k}^{(i)}$
 - 6: **end for**
 - 7: **end for**
 - 8: All-reduce step: $\mathbf{x}_{t,\tau} = \frac{1}{n} \sum_{i=1}^n \mathbf{x}_{t,\tau}^{(i)}$.
 - 9: Update global parameter:

$$\mathbf{u}_{t+1} \leftarrow \beta_1 \mathbf{m}_t + \frac{1 - \beta_1}{\gamma_t} (\mathbf{x}_{t,0} - \mathbf{x}_{t,\tau})$$

$$\mathbf{x}_{t+1,0} \leftarrow \mathbf{x}_{t,0} - \eta \gamma (\text{sign}(\mathbf{u}_{t+1}) + \lambda \mathbf{x}_{t,0})$$
 - 10: Update momentum:

$$\mathbf{m}_{t+1} = \beta_2 \mathbf{m}_t + \frac{1 - \beta_2}{\gamma_t} (\mathbf{x}_{t,0} - \mathbf{x}_{t,\tau})$$
 - 11: Synchronize over all workers:

$$\forall i \in [n], \mathbf{x}_{t+1,0}^{(i)} \leftarrow \mathbf{x}_{t+1,0}$$
 - 12: **end for**
 - 13: **return** $\mathbf{x}_{T,0}$
-

Global sign momentum step. The updates (5)-(7) offer a flexible configuration for the global sign momentum step. Specifically, when $\beta_2 > \beta_1$, the current $(\mathbf{x}_{t,0} - \mathbf{x}_{t,\tau})$ takes on a larger weight in the exponential moving average, similar to classical momentum as in SlowMo. This adjustment in momentum can lead to further

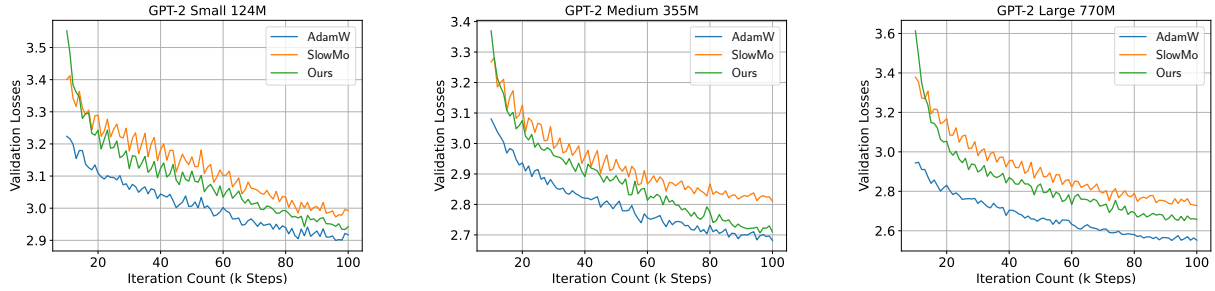


Figure 1: Validation loss curves for communication interval $\tau = 12$.

acceleration, as studied by [Shi et al. \(2022\)](#). Additionally, the decoupled weight decay in (6) is similar to the weight decay used in AdamW, making it more advantageous than Adam.

Distributed optimizer. We note that Algorithm 1 can be seamlessly integrated with the ZERO-series distributed optimizer ([Rajbhandari et al., 2020](#)) to handle large models. Consider a layered distributed optimization strategy: GPUs on a single node can be treated as a joint worker, utilizing a distributed optimizer like ZERO2 for local updates of the base optimizer, while the global buffers $\mathbf{x}_{t,0}$ and $\mathbf{m}_{t,0}$ are distributed across nodes. This approach allows more frequent communication for local updates to leverage faster intra-node communication, such as NVLinks.

Table 1: Model configurations and peak learning rates

	Size	Embedding dimension	# of heads	Depth	Peak LR
Small	125M	768	12	12	5e-4
Medium	355M	1024	16	24	2e-4
Large	770M	1280	20	36	2e-4

3 Convergence analysis

We provide some theoretical justifications on the convergence of Algorithm 1 under some regular conditions. Let $f_i(\mathbf{x}) := \mathbb{E}_{\boldsymbol{\xi}^{(i)} \sim \mathcal{D}_i} F_i(\mathbf{x}, \boldsymbol{\xi}^{(i)})$. We make the following assumptions on local functions.

Assumption 1. Each local function f_i is differentiable and $\forall \mathbf{x}, \mathbf{y} \in \mathbb{R}^d, \|\nabla f_i(\mathbf{x}) - \nabla f_i(\mathbf{y})\| \leq L\|\mathbf{x} - \mathbf{y}\|$ for some $L > 0$.

Let $\mathbb{E}_{t,k}$ denote the conditional expectation given all the historical randomness up to iteration (t, k) . We define the virtual global averages:

$$\mathbf{x}_{t,k} = \frac{1}{n} \sum_{i=1}^n \mathbf{x}_{t,k}^{(i)}, \quad \mathbf{d}_{t,k} = \frac{1}{n} \sum_{i=1}^n \mathbf{d}_{t,k}^{(i)}.$$

We assume that the average update direction $\mathbf{d}_{t,k}$ has bounded variance.

Assumption 2. There exists some $\zeta > 0$ such that $\mathbb{E}[\|\mathbf{d}_{t,k} - \mathbb{E}_{t,k}[\mathbf{d}_{t,k}]\|^2] \leq \zeta^2$.

Similar to [Sun et al. \(2023\)](#), we assume that update directions of base optimizers are uniformly bounded throughout the optimization process.

Assumption 3. *The local update direction of each local base optimizer is bounded at all iteration (t, k) : $\forall (t, k), \forall i \in [n], \|\mathbf{d}_{t,k}^{(i)}\|^2 \leq R^2$ for some $R > 0$.*

Randomized sign operator. In our analysis, we approximate the sign operator with a randomized analog. For any vector $\mathbf{v} = [v_1, \dots, v_d]^\top \in \mathbb{R}^d$ such that $\|\mathbf{v}\| \leq B$, we use the randomized sign operator $\mathcal{S}_r(\mathbf{v})$, where the j -th component is defined as:

$$[\mathcal{S}_r(\mathbf{v})]_j = \begin{cases} -\text{sign}(v_j), & \text{with probability (w.p.) } \frac{1}{2} - \frac{|v_j|}{2B}, \\ \text{sign}(v_j), & \text{w.p. } \frac{1}{2} + \frac{|v_j|}{2B}. \end{cases} \quad (8)$$

Or alternatively,

$$[\mathcal{S}_r(\mathbf{v})]_j = \begin{cases} 0, & \text{w.p. } 1 - \frac{|v_j|}{B}, \\ \text{sign}(v_j), & \text{w.p. } \frac{|v_j|}{B}. \end{cases} \quad (9)$$

We use these randomized sign operators as a linear and continuous analog of the original sign operator in expectation. Let $\mathbb{E}_{\mathcal{S}}$ denote the expectation taken over the randomness of the randomized sign operator, we have the following property.

Lemma 1. *For a random vector $\mathbf{v} \in \mathbb{R}^d$ that satisfies $\|\mathbf{v}\| \leq B$ almost surely, we have $\mathbb{E}_{\mathcal{S}}[\mathbf{v}] = \mathbf{v}/B$, and $\mathbb{E}_{\mathcal{S}}[\|\mathcal{S}_r(\mathbf{v}) - \mathbf{v}/B\|^2] \leq d$.*

With the above linearization in expectation, we establish a general convergence for some specific instances of Algorithm 1. Proofs of all theorems are deferred to the Appendix.

Theorem 1. *Let Assumptions 1, 2, and 3 hold. Run Algorithm 1 by approximating sign with \mathcal{S}_r in (8) or (9) with $B = \tau R$. Take local learning rate $\gamma = \frac{R}{\eta} \sqrt{\frac{n\tau}{T}}$, weight decay $\lambda = 0$, and momentum coefficients $\beta_1 = \beta_2 = \beta \in [0, 1)$. When the outer iterations number $T \geq 4nL^2 [4(\tau - 1)(\frac{\tau R}{\eta} - 1)^2 + \frac{8\tau\beta^2}{(1-\beta)^2} + 1]$, the iterates $\{\mathbf{x}_{t,k}\}$ generated from Algorithm 1 satisfy that*

$$\begin{aligned} \frac{1}{\tau T} \sum_{t=0}^{T-1} \sum_{k=0}^{\tau-1} \mathbb{E} \|\nabla f(\mathbf{x}_{t,k})\|^2 &\leq \frac{2(f(\mathbf{x}_{0,0}) - f_*)}{\sqrt{n\tau T}} \\ &+ \underbrace{\frac{1}{\tau T} \sum_{t=0}^{T-1} \sum_{k=0}^{\tau-1} \mathbb{E} [\|\nabla f(\mathbf{x}_{t,k}) - \mathbb{E}[\mathbf{d}_{t,k}]\|^2]}_{\text{Effect of base optimizer}} + \zeta^2 L \sqrt{\frac{n}{\tau T}} \\ &+ \frac{4nL^2\zeta^2}{T} \left[\left(\frac{\tau R}{\eta} - 1\right)^2 + \frac{2\beta^2}{1-\beta^2} \right] + dLR^2 \sqrt{\frac{n\tau}{T}}. \end{aligned}$$

Theorem 1 provides a general convergence guarantee for the simple sign momentum case of Algorithm 1. The convergence rate depends on the *effect of base optimizer*, which can measure both gradient heterogeneity across workers and stochastic gradient bias. We next specialize to the case where the base optimizer is SGD.

Theorem 2. *Let Assumptions 1, 3 hold, and in addition assume that:*

- (a) *the local update direction $\mathbf{d}_{t,k}^{(i)} = \nabla F_i(\mathbf{x}_{t,k}, \boldsymbol{\xi}_{t,k}^{(i)})$, and $\forall \mathbf{x} \in \mathbb{R}^d, \mathbb{E}_{\boldsymbol{\xi}^{(i)} \sim \mathcal{D}_i} [\|\nabla F_i(\mathbf{x}, \boldsymbol{\xi}^{(i)}) - \nabla f_i(\mathbf{x})\|^2] \leq \sigma^2$ for some $\sigma > 0$;*
- (b) *$\forall \mathbf{x} \in \mathbb{R}^d, (1/n) \sum_{i=1}^n \|\nabla f(\mathbf{x}) - \nabla f_i(\mathbf{x})\|^2 \leq \delta^2$ for some $\delta > 0$.*

Then, by approximating sign with randomized operator \mathcal{S}_r and using parameters $\gamma, \eta, \lambda, \beta_1, \beta_2$ and T as in Theorem 1, we have $\frac{1}{\tau T} \sum_{t=0}^{T-1} \sum_{k=0}^{\tau-1} \mathbb{E} [\|\nabla f(\mathbf{x}_{t,k})\|^2] = O(1/\sqrt{\tau T})$.

Remark 1. We compare the instance in Theorem 2 with a similar algorithm, Federated Majority Vote signSGD with Stochastic Simple Momentum (Federated MV-sto-signSGD-SIM), analyzed by Sun et al. (2023). First, our algorithm uses aggregated local differences ($\mathbf{x}_{t,0} - \mathbf{x}_{t,\tau}$) for a global momentum update while MV-sto-signSGD-SIM uses local stochastic gradients to update local momentum before applying sign based majority vote. Second, Sun et al. (2023) prove its convergence to an $O(dR)$ neighborhood under the same Assumption 3, while Theorem 2, by using a simplified randomized sign \mathcal{S}_r , shows convergences to 0 with rate $O(1/\sqrt{T})$.

4 Experiments

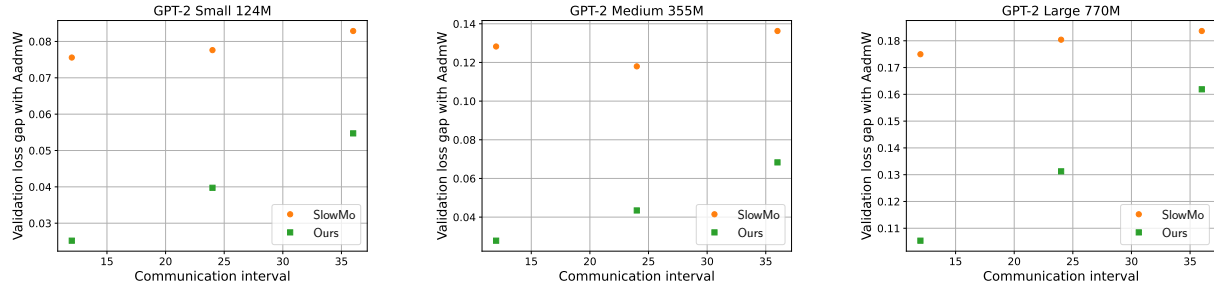


Figure 2: Final validation loss gaps with AdamW under different communication intervals.

We evaluate Algorithm 1 on auto-regressive language modeling using GPT-2 (Radford et al., 2019), with model sizes ranging from 125M to 770M parameters, trained from scratch on the OpenWebText dataset (Gokaslan et al., 2019). Following standard practice, we set the context length of GPT-2 to 1024 tokens. We consider three versions of GPT-2: 125M (Small), 355M (Medium), and 770M (Large) parameters, with configurations as detailed in Table 1.

Baselines. We benchmark our empirical performance using AdamW. AdamW is the dominant optimizer for the pre-training of Transformers (Liu et al., 2024), and we use its results under synchronized gradient communication as the baseline. We compare the performance gap, measured in validation losses, of Algorithm 1, and SlowMo when base optimizers in both framework are set as AdamW in that SlowMo with AdamW is among the best performing local updating methods (Sun et al., 2024). We omit the comparison with local AdamW with periodic averaging due to its poor performance.

Implementations. We set the total batch size to 480 for all algorithms and run each for 100k steps. In this setup, we fine-tune the recommended parameters for AdamW (both for the base optimizer AdamW in Algorithm 1 and SlowMo): $\beta_1 = 0.9$, $\beta_2 = 0.95$, and a cosine learning rate schedule (Loshchilov and Hutter, 2016) with a 2k-step warm-up. The peak learning rate (LR) is specified in Table 1, and the final LR is set to $0.05 \times$ the peak LR. For the global sign momentum step in Algorithm 1, we apply the recommended Lion parameters: $\beta_1 = 0.95$, $\beta_2 = 0.98$, and $\lambda = 0.1$ (Liu et al., 2024). We tune the momentum coefficient and global LR for SlowMo, and the global LR for Algorithm 1. Performance is tested on three different sizes of GPT-2 models across varying numbers of workers.

Parameter tuning. We perform the following model pre-training.

1. GPT-2 Small on 8 workers. We tune SlowMo with momentum coefficients in $\{0.2, 0.4, 0.5, 0.6, 0.7, 0.8, 0.9\}$, and global LR in $\{0.5, 1, 2\}$; and we tune global LR of Algorithm 1 in $\{0.1, 0.5, 0.8, 1.2, 1.5\}$.
2. GPT-2 Medium on 8 workers. For SlowMo, we use the best performing momentum coefficient in GPT-2 Small training, and tune global LR in $\{0.5, 0.8, 1.0\}$. For Algorithm 1, we tune global LR in $\{0.5, 0.8, 1.0, 1.2, 1.5, 2.0\}$.

- GPT-2 Large on 16 workers. SlowMo momentum coefficient is chosen from $\{0.5, 0.6\}$ and global LR is from $\{0.5, 1.0\}$. Algorithm 1 uses the best global LR in $\{0.5, 0.8, 1.0, 1.2\}$.

Improved performance. In Figure 1, we present the validation loss curves during the pre-training of the three GPT-2 models, with the communication interval τ set to 12. In all three experiments, our method consistently outperforms SlowMo by a significant margin. Notably, despite achieving a $12\times$ communication reduction, our approach demonstrates only a small final validation loss gap compared to AdamW under perfect synchronized communication, particularly for GPT-2 Small and GPT-2 Medium.

On the effects of communication interval τ . In Figure 2, we illustrate the performance gaps, quantified by increased final validation losses, for the three model pre-training setups under different communication intervals, $\tau = 12, 24, 36$. The scatter plots show that across all model sizes and communication intervals, our method consistently outperforms SlowMo, highlighting the advantages of sign momentum over standard momentum. Additionally, we observe that as τ increases, the performance gap between our method and SlowMo narrows. Nevertheless, a $10\times$ or $20\times$ reduction in communication would still offer substantial savings in practical distributed training scenarios.

4.1 Ablation studies

We conducted several ablation studies to explore the factors contributing to the effectiveness of sign momentum. In all these studies, we used the AdamW optimizer as the base optimizer, as described in the previous section.

Lookahead and signed Lookahead optimizer. We begin by testing whether momentum and signed momentum improve local updating methods in the case of a single worker. To do this, we configure Algorithm 1 with $n = 1$, $\beta_1 = \beta_2 = \beta$, and $\lambda = 0$, reducing it to the signed Lookahead optimizer. Upon that, by replacing (6) with $\mathbf{x}_{t+1,0} = \mathbf{x}_{t,0} - \eta\gamma_t\mathbf{u}_{t+1}$, we recover the Lookahead optimizer (Zhang et al., 2019). In Figure 3, we plot the validation loss curves during GPT-2 Medium pre-training with communication interval $\tau = 48$. The results show that the Lookahead optimizer consistently outperforms the base optimizer AdamW across various choices of the momentum coefficient β , highlighting the critical role of momentum in training Transformers. Additionally, as shown in Figure 4, the signed Lookahead optimizer also demonstrates improvements over AdamW, albeit with more fluctuations, likely due to the nature of the signed updates. Through these experiments, we demonstrate that both momentum and signed momentum are effective when $n = 1$.

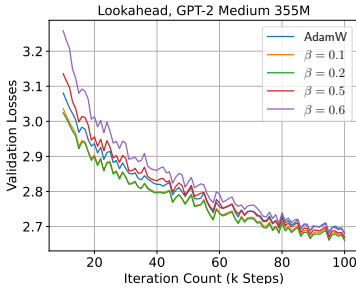


Figure 3: Lookahead optimizer: global LR= 1, $\tau = 48$.

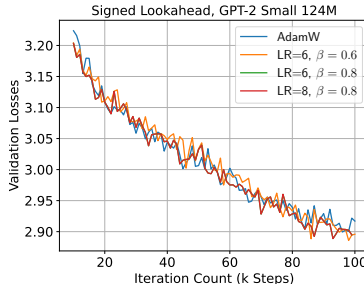


Figure 4: Signed Lookahead optimizer: $\tau = 24$.

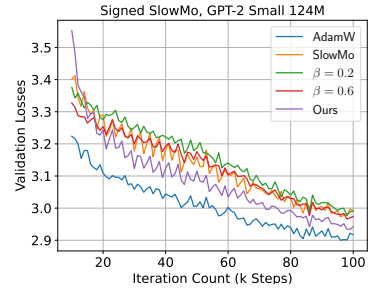


Figure 5: Signed SlowMo: global LR= 3, $\tau = 12$.

Signed SlowMo. We now consider the case with multiple workers, i.e., when $n > 1$. In this setting, we define signed SlowMo by setting $\beta_1 = \beta_2 = \beta$, and modifying the updates in (5) and (6) as follows:

$$\mathbf{u}_{t+1} = \beta_1 \mathbf{m}_t + \frac{1 - \beta_1}{\gamma_t} \text{sign}(\mathbf{x}_{t,0} - \mathbf{x}_{t,\tau}),$$

$$\mathbf{x}_{t+1,0} = \mathbf{x}_{t,0} - \eta\gamma_t\mathbf{u}_{t+1}.$$

We use signed SlowMo to pre-train the GPT-2 Small model with a communication interval of $\tau = 12$. As shown in Figure 5, signed SlowMo achieves better final validation losses compared to SlowMo, showing the efficacy of incorporating sign momentum. However, it still underperforms compared to our proposed method, which we hypothesize is due to the acceleration effects provided by using $\beta_2 > \beta_1$.

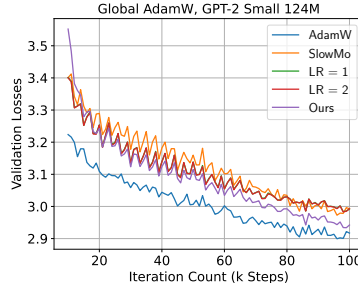


Figure 6: Global step that mimics AdamW: $\tau = 12$.

Adaptive global update. We further compare the global sign momentum method with a global step that mimics AdamW (see Appendix for a description). Balles and Hennig (2018) show that Adam can be regarded as sign momentum with adaptive learning rate depending on relative variance. Our empirical results, as plotted in Figure 6, show that its performance is only comparable with SlowMo, partially indicating that this adaptivity brings limited benefits when used as the global step of local updating methods. We defer its detailed description of this comparisons to the Appendix.

5 Conclusion and Discussions

In this paper, we have introduced a new framework for distributed sign momentum with local updates, integrating sign momentum with a communication-efficient local update approach. The framework is flexible, accommodating a variety of off-the-shelf base optimizers. Empirical results from training GPT-2 models of various sizes consistently show improvements over baseline algorithms, validating the effectiveness of our approach. Additionally, a series of ablation studies highlights the impact of sign momentum in different scenarios. We also provide theoretical justification for the framework by utilizing a randomized version of the sign operator and proving an $O(1/\sqrt{T})$ convergence rate when using SGD as the base optimizer. To the best of our knowledge, this framework is a novel contribution to the literature.

Future directions include evaluating the performance of the proposed method on training vision models, such as Vision Transformers (Dosovitskiy, 2020), and investigating the convergence of Algorithm 1 under broader parameter settings and with the real sign operator.

References

- Mahmoud Assran, Nicolas Loizou, Nicolas Ballas, and Mike Rabbat. Stochastic gradient push for distributed deep learning. In *International Conference on Machine Learning*, pages 344–353. PMLR, 2019.
- Lukas Balles and Philipp Hennig. Dissecting adam: The sign, magnitude and variance of stochastic gradients. In *International Conference on Machine Learning*, pages 404–413. PMLR, 2018.
- Jeremy Bernstein, Yu-Xiang Wang, Kamyar Azizzadenesheli, and Animashree Anandkumar. signsgd: Compressed optimisation for non-convex problems. In *International Conference on Machine Learning*, pages 560–569. PMLR, 2018.
- Jeremy Bernstein, Jiawei Zhao, Kamyar Azizzadenesheli, and Anima Anandkumar. signsgd with majority vote is communication efficient and fault tolerant. In *International Conference on Learning Representations*, 2019.
- Kai Chen and Qiang Huo. Scalable training of deep learning machines by incremental block training with intra-block parallel optimization and blockwise model-update filtering. In *2016 IEEE International Conference on Acoustics, Speech and Signal Processing (ICASSP)*, pages 5880–5884. IEEE, 2016.
- Lizhang Chen, Bo Liu, Kaizhao Liang, et al. Lion secretly solves a constrained optimization: As lyapunov predicts. In *The Twelfth International Conference on Learning Representations*, 2024a.
- Xiangning Chen, Chen Liang, Da Huang, Esteban Real, Kaiyuan Wang, Hieu Pham, Xuanyi Dong, Thang Luong, Cho-Jui Hsieh, Yifeng Lu, et al. Symbolic discovery of optimization algorithms. *Advances in neural information processing systems*, 36, 2024b.
- Jeffrey Dean, Greg Corrado, Rajat Monga, Kai Chen, Matthieu Devin, Mark Mao, Marc’auelio Ranzato, Andrew Senior, Paul Tucker, Ke Yang, et al. Large scale distributed deep networks. *Advances in neural information processing systems*, 25, 2012.
- Alexey Dosovitskiy. An image is worth 16x16 words: Transformers for image recognition at scale. *arXiv preprint arXiv:2010.11929*, 2020.
- Aaron Gokaslan, Vanya Cohen, Ellie Pavlick, and Stefanie Tellex. Openwebtext corpus. 2019.
- Eduard Gorbunov, Konstantin P Burlachenko, Zhize Li, and Peter Richtárik. Marina: Faster non-convex distributed learning with compression. In *International Conference on Machine Learning*, pages 3788–3798. PMLR, 2021a.
- Eduard Gorbunov, Filip Hanzely, and Peter Richtárik. Local sgd: Unified theory and new efficient methods. In *International Conference on Artificial Intelligence and Statistics*, pages 3556–3564. PMLR, 2021b.
- Zhanhong Jiang, Aditya Balu, Chinmay Hegde, and Soumik Sarkar. Collaborative deep learning in fixed topology networks. *Advances in Neural Information Processing Systems*, 30, 2017.
- Peter H Jin, Qiaochu Yuan, Forrest Iandola, and Kurt Keutzer. How to scale distributed deep learning? *arXiv preprint arXiv:1611.04581*, 2016.
- Sai Praneeth Karimireddy, Quentin Rebjock, Sebastian Stich, and Martin Jaggi. Error feedback fixes signsgd and other gradient compression schemes. In *International Conference on Machine Learning*, pages 3252–3261. PMLR, 2019.
- Sai Praneeth Karimireddy, Satyen Kale, Mehryar Mohri, Sashank Reddi, Sebastian Stich, and Ananda Theertha Suresh. Scaffold: Stochastic controlled averaging for federated learning. In *International conference on machine learning*, pages 5132–5143. PMLR, 2020.

- Ahmed Khaled, Konstantin Mishchenko, and Peter Richtárik. Tighter theory for local sgd on identical and heterogeneous data. In *International Conference on Artificial Intelligence and Statistics*, pages 4519–4529. PMLR, 2020.
- Diederik P Kingma. Adam: A method for stochastic optimization. *arXiv preprint arXiv:1412.6980*, 2014.
- Frederik Kunstner, Jacques Chen, Jonathan Wilder Lavington, and Mark Schmidt. Noise is not the main factor behind the gap between sgd and adam on transformers, but sign descent might be. *arXiv preprint arXiv:2304.13960*, 2023.
- Xiangru Lian, Ce Zhang, Huan Zhang, Cho-Jui Hsieh, Wei Zhang, and Ji Liu. Can decentralized algorithms outperform centralized algorithms? a case study for decentralized parallel stochastic gradient descent. *Advances in neural information processing systems*, 30, 2017.
- Tao Lin, Sebastian U Stich, Kumar Kshitij Patel, and Martin Jaggi. Don’t use large mini-batches, use local sgd. In *International Conference on Learning Representations*, 2020.
- Hong Liu, Zhiyuan Li, David Leo Wright Hall, Percy Liang, and Tengyu Ma. Sophia: A scalable stochastic second-order optimizer for language model pre-training. In *The Twelfth International Conference on Learning Representations*, 2024.
- I Loshchilov. Decoupled weight decay regularization. *arXiv preprint arXiv:1711.05101*, 2017.
- Ilya Loshchilov and Frank Hutter. Sgdr: Stochastic gradient descent with warm restarts. *arXiv preprint arXiv:1608.03983*, 2016.
- Yucheng Lu, Conglong Li, Minjia Zhang, Christopher De Sa, and Yuxiong He. Maximizing communication efficiency for large-scale training via 0/1 adam. In *The Eleventh International Conference on Learning Representations*, 2023.
- Brendan McMahan, Eider Moore, Daniel Ramage, Seth Hampson, and Blaise Aguera y Arcas. Communication-efficient learning of deep networks from decentralized data. In *Artificial intelligence and statistics*, pages 1273–1282. PMLR, 2017.
- Yurii Nesterov. A method for solving a convex programming problem with convergence rate $o(1/k^2)$. In *Soviet Mathematics. Doklady*, volume 27, pages 367–372, 1983.
- Boris T Polyak. Some methods of speeding up the convergence of iteration methods. *Ussr computational mathematics and mathematical physics*, 4(5):1–17, 1964.
- Alec Radford, Jeffrey Wu, Rewon Child, David Luan, Dario Amodei, Ilya Sutskever, et al. Language models are unsupervised multitask learners. *OpenAI blog*, 1(8):9, 2019.
- Samyam Rajbhandari, Jeff Rasley, Olatunji Ruwase, and Yuxiong He. Zero: Memory optimizations toward training trillion parameter models. In *SC20: International Conference for High Performance Computing, Networking, Storage and Analysis*, pages 1–16. IEEE, 2020.
- Herbert Robbins and Sutton Monro. A stochastic approximation method. *The annals of mathematical statistics*, pages 400–407, 1951.
- Frank Seide, Hao Fu, Jasha Droppo, Gang Li, and Dong Yu. 1-bit stochastic gradient descent and its application to data-parallel distributed training of speech dnns. In *Interspeech*, volume 2014, pages 1058–1062. Singapore, 2014.
- Bin Shi, Simon S Du, Michael I Jordan, and Weijie J Su. Understanding the acceleration phenomenon via high-resolution differential equations. *Mathematical Programming*, pages 1–70, 2022.

- Tao Sun, Qingsong Wang, Dongsheng Li, and Bao Wang. Momentum ensures convergence of signsgd under weaker assumptions. In *International Conference on Machine Learning*, pages 33077–33099. PMLR, 2023.
- Weigao Sun, Zhen Qin, Weixuan Sun, Shidi Li, Dong Li, Xuyang Shen, Yu Qiao, and Yiran Zhong. Co2: Efficient distributed training with full communication-computation overlap. *arXiv preprint arXiv:2401.16265*, 2024.
- Ilya Sutskever, James Martens, George Dahl, and Geoffrey Hinton. On the importance of initialization and momentum in deep learning. In *International conference on machine learning*, pages 1139–1147. PMLR, 2013.
- A Vaswani. Attention is all you need. *Advances in Neural Information Processing Systems*, 2017.
- Jianyu Wang, Vinayak Tantia, Nicolas Ballas, and Michael Rabbat. Slowmo: Improving communication-efficient distributed sgd with slow momentum. *arXiv preprint arXiv:1910.00643*, 2019.
- Jianyu Wang, Qinghua Liu, Hao Liang, Gauri Joshi, and H Vincent Poor. Tackling the objective inconsistency problem in heterogeneous federated optimization. *Advances in neural information processing systems*, 33: 7611–7623, 2020.
- Cong Xie, Shuai Zheng, Sanmi Koyejo, Indranil Gupta, Mu Li, and Haibin Lin. Cser: Communication-efficient sgd with error reset. *Advances in Neural Information Processing Systems*, 33:12593–12603, 2020.
- Hao Yu, Rong Jin, and Sen Yang. On the linear speedup analysis of communication efficient momentum sgd for distributed non-convex optimization. In *International Conference on Machine Learning*, pages 7184–7193. PMLR, 2019.
- Michael Zhang, James Lucas, Jimmy Ba, and Geoffrey E Hinton. Lookahead optimizer: k steps forward, 1 step back. *Advances in neural information processing systems*, 32, 2019.

A Optimizer descriptions

In this section, we provide detailed descriptions of the algorithms referenced in the main text. In the absence of local steps, we present the pseudocode for Polyak’s Momentum (Algorithm 3), AdamW (Algorithm 2), and Lion (Algorithm 4). We denote the stochastic gradient computed at \mathbf{x} using random samples $\boldsymbol{\xi}$ as $\nabla f(\mathbf{x}, \boldsymbol{\xi})$, where \mathbf{x} and $\boldsymbol{\xi}$ are defined based on the given context. For distributed algorithms with local steps, we give the pseudocode of SlowMo (Algorithm 5) and Federated Majority Vote signSGD with Stochastic Simple Momentum (Federated MV-sto-signSGD-SIM in Algorithm 6).

Algorithm 2 AdamW, Adam (Kingma, 2014) with decoupled weight decay proposed by Loshchilov (2017). Component-wise vector multiplication $\mathbf{g}_t^2 = \mathbf{g}_t \odot \mathbf{g}_t$, and $\sqrt{\widehat{\mathbf{v}}_t}$ means component-wise square root.

Require: Initialization \mathbf{x}_0 , momentum coefficients β_1, β_2 ; weight decay λ ; learning rate η ; $\epsilon = 10^{-8}$

$\mathbf{m}_0 \leftarrow \mathbf{0}, \mathbf{v}_0 \leftarrow \mathbf{0}$

for $t = 0$ to $T - 1$ **do**

 Stochastic gradient: $\mathbf{g}_t \leftarrow \nabla f(\mathbf{x}_t, \boldsymbol{\xi}_t)$

 Momentum updates:

$\mathbf{m}_{t+1} \leftarrow \beta_1 \mathbf{m}_t + (1 - \beta_1) \mathbf{g}_t$

$\mathbf{v}_{t+1} \leftarrow \beta_2 \mathbf{v}_t + (1 - \beta_2) \mathbf{g}_t^2$

 Bias-corrections:

$\widehat{\mathbf{m}}_{t+1} \leftarrow \mathbf{m}_{t+1} / (1 - \beta_1^{t+1})$

$\widehat{\mathbf{v}}_{t+1} \leftarrow \mathbf{v}_{t+1} / (1 - \beta_2^{t+1})$

 Parameter update:

$\mathbf{x}_{t+1} \leftarrow \mathbf{x}_t - \eta \left(\frac{\widehat{\mathbf{m}}_{t+1}}{\sqrt{\widehat{\mathbf{v}}_{t+1} + \epsilon}} + \lambda \mathbf{x}_t \right)$

end for

return \mathbf{x}_T

Algorithm 3 Polyak’s Momentum (Polyak, 1964).

Require: Initialization \mathbf{x}_0 , momentum coefficient β , learning rate $\eta > 0$

1: $\mathbf{m}_0 \leftarrow \mathbf{0}$

2: **for** $t = 0$ to $T - 1$ **do**

3: Stochastic gradient: $\mathbf{g}_t \leftarrow \nabla f(\mathbf{x}_t, \boldsymbol{\xi}_t)$

4: Momentum update: $\mathbf{m}_{t+1} \leftarrow \beta \mathbf{m}_t + \mathbf{g}_t$

5: Parameter update: $\mathbf{x}_{t+1} \leftarrow \mathbf{x}_t - \eta \mathbf{m}_{t+1}$

6: **end for**

7: **Return** \mathbf{x}_T

Algorithm 4 Lion (Chen et al., 2024b).

Require: Initialization \mathbf{x}_0 ; momentum coefficients β_1, β_2 ; weight decay λ , learning rate η

1: $\mathbf{m}_0 \leftarrow \mathbf{0}$

2: **for** $t = 0$ to $T - 1$ **do**

3: Stochastic gradient: $\mathbf{g}_t \leftarrow \nabla f(\mathbf{x}_t, \boldsymbol{\xi}_t)$

4: Parameter update:

$\mathbf{u}_{t+1} \leftarrow \beta_1 \mathbf{m}_t + (1 - \beta_1) \mathbf{g}_t$

$\mathbf{x}_{t+1} \leftarrow \mathbf{x}_t - \eta (\text{sign}(\mathbf{u}_{t+1}) + \lambda \mathbf{x}_t)$

5: Momentum update:

$\mathbf{m}_{t+1} \leftarrow \beta_2 \mathbf{m}_t + (1 - \beta_2) \mathbf{g}_t$

6: **end for**

7: **Return** \mathbf{x}_T

B Additional proofs

B.1 Proof of Theorem 1

B.1.1 Proof of Lemma 1

Proof. For \mathcal{S}_r defined in (8) and (9), it can be readily verified that if $\|\mathbf{v}\| \leq B$, $\mathbb{E}_{\mathcal{S}}[\mathcal{S}(\mathbf{v})] = \mathbf{v}/B$. Then,

$$\mathbb{E}_{\mathcal{S}}[\|\mathcal{S}_r(\mathbf{v}) - \frac{\mathbf{v}}{B}\|^2] = \mathbb{E}_{\mathcal{S}}[\|\mathcal{S}_r(\mathbf{v}) - \mathbb{E}_{\mathcal{S}}[\mathcal{S}_r(\mathbf{v})]\|^2] = \mathbb{E}_{\mathcal{S}}[\|\mathcal{S}_r(\mathbf{v})\|^2] - \frac{\|\mathbf{v}\|^2}{B^2} \leq d,$$

where the last step follows from that $\mathcal{S}_r(\mathbf{v})$ ’s component is either 0 or ± 1 . \square

Algorithm 5 SlowMo, a general framework that combines local steps and global momentum step (Wang et al., 2019). Worker i 's updating direction of base optimizer at iteration (t, k) is denoted as $\mathbf{d}_{t,i}^{(i)}$.

Require: Initialization $\mathbf{x}_{0,0}$; base optimizer learning rate γ_t ; inner loop steps τ ; global learning rate α ; initial momentum $\mathbf{u}_0 = \mathbf{0}$

for $t = 0$ to $T - 1$ at worker i in parallel **do**

for $k = 0$ to $\tau - 1$ **do**

 Base optimizer step: $\mathbf{x}_{t,k+1}^{(i)} \leftarrow \mathbf{x}_{t,k}^{(i)} - \gamma_t \mathbf{d}_{t,k}^{(i)}$

end for

 Exact averaging: $\mathbf{x}_{t,\tau} \leftarrow \frac{1}{n} \sum_{i=1}^n \mathbf{x}_{t,\tau}^{(i)}$

 Update slow momentum:

$\mathbf{u}_{t+1} \leftarrow \beta \mathbf{u}_t + \frac{1}{\gamma_t} (\mathbf{x}_{t,0} - \mathbf{x}_{t,\tau})$

 Update outer iterate: $\mathbf{x}_{t+1,0} \leftarrow \mathbf{x}_{t,0} - \alpha \gamma_t \mathbf{u}_{t+1}$

end for

return $\mathbf{x}_{T,0}$

Algorithm 6 Federated MV-sto-signSGD-SIM (Sun et al., 2023). The randomized sign operator \mathcal{S}_r is as defined in (8).

Require: Iterate initialization $\mathbf{x}_{-1} = \mathbf{x}_0 = \mathbf{0}$, momentum initialization $\mathbf{m}_0 = \mathbf{0}$, momentum coefficient $\beta \in [0, 1)$, local learning rate γ , inner loop steps τ , outer momentum coefficient α , global learning rate η , the uniform ℓ_2 norm bound on stochastic gradient B

- 1: **for** $t = 0$ to $T - 1$ **do**
- 2: $\mathbf{y}_t \leftarrow \mathbf{x}_t + \alpha(\mathbf{x}_t - \mathbf{x}_{t-1})$
- 3: **for** worker $i = 1$ to n in parallel **do**
- 4: $\mathbf{z}_{t,0}^{(i)} \leftarrow \mathbf{y}_t$
- 5: **for** $k = 0$ to $\tau - 1$ **do**
- 6: $\mathbf{z}_{t,k+1}^{(i)} \leftarrow \mathbf{z}_{t,k}^{(i)} - \gamma \nabla f_i(\mathbf{z}_{t,k}^{(i)}, \boldsymbol{\xi}_{t,k}^{(i)})$
- 7: **end for**
- 8: $\mathbf{y}_t^{(i)} \leftarrow \mathbf{z}_{t,\tau}^{(i)}$
- 9: $\mathbf{m}_{t+1}^{(i)} \leftarrow \beta \mathbf{m}_t^{(i)} + (1 - \beta) \nabla f_i(\mathbf{y}_t^{(i)}, \boldsymbol{\xi}_t^{(i)})$
- 10: **end for**
- 11: Communicate and majority vote:

$$\mathbf{x}_{t+1} \leftarrow \mathbf{x}_t - \eta \text{sign}\left(\sum_{i=1}^n \mathcal{S}_r(\mathbf{m}_i^{(t+1)})\right)$$
- 12: **end for**
- 13: **Return** \mathbf{x}_T

B.1.2 Virtual iterates

Recall that at iteration (t, k) , the local updates are given by $\mathbf{x}_{t,k+1}^{(i)} = \mathbf{x}_{t,k}^{(i)} - \gamma \mathbf{d}_{t,k}^{(i)}$. We define the global averages:

$$\mathbf{d}_{t,k} := \frac{1}{n} \sum_{i=1}^n \mathbf{d}_{t,k}^{(i)}, \quad \mathbf{x}_{t,k} := \frac{1}{n} \sum_{i=1}^n \mathbf{x}_{t,k}^{(i)}.$$

Then, one has

$$\mathbf{x}_{t,k} = \mathbf{x}_{t,0} - \gamma \sum_{i=0}^{k-1} \mathbf{d}_{t,i}.$$

In the global update step,

$$\mathbf{x}_{t+1,0} = \mathbf{x}_{t,0} - \eta\gamma \mathcal{S}_r(\mathbf{m}_{t+1}) = \mathbf{x}_{t,0} - \eta\gamma \mathcal{S}_r\left(\beta \mathbf{m}_t + (1-\beta) \sum_{i=0}^{\tau-1} \mathbf{d}_{t,i}\right).$$

By Assumption 3 and Jensen's inequality, we have $\|\mathbf{d}_{t,i}\| \leq R$ almost surely (a.s.), and thus $\|\sum_{i=0}^{\tau-1} \mathbf{d}_{t,i}\| \leq \tau R$ a.s.. Further, \mathbf{m}_{t+1} is a convex combination of \mathbf{m}_t and $\sum_{i=0}^{\tau-1} \mathbf{d}_{t,i}$ with $\mathbf{m}_0 = \mathbf{0}$, then one can readily show that $\|\mathbf{m}_t\| \leq \tau R$ for all $t \geq 0$. Using \mathcal{S}_r with $B = \tau R$ and taking total expectation, we have

$$\begin{aligned} \mathbb{E}[\mathbf{x}_{t+1,0}] &= \mathbb{E}[\mathbf{x}_{t,0}] - \eta\gamma \mathbb{E}[\mathcal{S}_r(\mathbf{m}_{t+1})] \\ &= \mathbb{E}[\mathbf{x}_{t,0}] - \frac{\eta\gamma}{\tau R} \mathbb{E}[\mathbf{m}_{t+1}] \\ &= \mathbb{E}[\mathbf{x}_{t,0}] - \frac{\eta\gamma}{\tau R} \left(\beta \mathbb{E}[\mathbf{m}_t] + (1-\beta) \sum_{i=0}^{\tau-1} \mathbb{E}[\mathbf{d}_{t,i}] \right) \end{aligned} \quad (10)$$

We define the following auxiliary iterates $\mathbf{y}_{t,k}$ at iteration (t, k) for $k = 0, \dots, \tau$:

$$\mathbf{y}_{t,k} := \mathbf{x}_{t,0} - \frac{\eta\gamma}{\tau R(1-\beta)} \left[\beta \mathbf{m}_t + (1-\beta) \sum_{i=0}^{k-1} \mathbf{d}_{t,i} \right], \quad (11)$$

where we use the convention $\sum_{i=0}^{-1} \mathbf{d}_{t,i} = \mathbf{0}$. From the definition in (11), we have the following relations for the virtual iterates $\{\mathbf{y}_{t,k}\}$:

$$\mathbf{y}_{t,k+1} = \mathbf{y}_{t,k} - \frac{\eta\gamma}{\tau R} \mathbf{d}_{t,k}, \quad \forall k = 0, \dots, \tau-1, \quad (12)$$

In addition, under total expectation one has,

$$\mathbb{E}[\mathbf{y}_{t,\tau}] = \mathbb{E}[\mathbf{x}_{t,0}] - \frac{\eta\gamma}{\tau R(1-\beta)} \mathbb{E}[\mathbf{m}_{t+1}] \stackrel{(10)}{=} \mathbb{E}[\mathbf{x}_{t+1,0}] - \frac{\eta\gamma\beta}{\tau R(1-\beta)} \mathbb{E}[\mathbf{m}_{t+1}] = \mathbb{E}[\mathbf{y}_{t+1,0}]. \quad (13)$$

B.1.3 Decent Lemma

Let $\mathbb{E}_{t,k}$ denote the conditional expectation given history up to time (t, k) , and $\mathbb{E}_{\mathcal{S}}$ denote the expectation over the random sign operator \mathcal{S}_r . Since each f_i is L -smooth, the function f is also L -smooth. We have for $k = 0, \dots, \tau-1$,

$$\mathbb{E}_{t,k}[f(\mathbf{y}_{t,k+1})] - f(\mathbf{y}_{t,k}) \leq -\frac{\eta\gamma}{\tau R} \langle \nabla f(\mathbf{y}_{t,k}), \mathbb{E}_{t,k}[\mathbf{d}_{t,k}] \rangle + \frac{L\eta^2\gamma^2}{2\tau^2 R^2} \mathbb{E}_{t,k}[\|\mathbf{d}_{t,k}\|^2]. \quad (14)$$

For the first term on the right hand side, we have

$$\begin{aligned}
& - \langle \nabla f(\mathbf{y}_{t,k}), \mathbb{E}_{t,k}[\mathbf{d}_{t,k}] \rangle \\
&= - \langle \nabla f(\mathbf{y}_{t,k}) - \nabla f(\mathbf{x}_{t,k}), \mathbb{E}_{t,k}[\mathbf{d}_{t,k}] \rangle - \langle \nabla f(\mathbf{x}_{t,k}), \mathbb{E}_{t,k}[\mathbf{d}_{t,k}] \rangle \\
&\leq \|\nabla f(\mathbf{y}_{t,k}) - \nabla f(\mathbf{x}_{t,k})\|^2 - \frac{1}{4} \|\mathbb{E}_{t,k}[\mathbf{d}_{t,k}]\|^2 - \frac{1}{2} \|\nabla f(\mathbf{x}_{t,k})\|^2 + \frac{1}{2} \|\nabla f(\mathbf{x}_{t,k}) - \mathbb{E}_{t,k}[\mathbf{d}_{t,k}]\|^2 \\
&\leq L^2 \|\mathbf{y}_{t,k} - \mathbf{x}_{t,k}\|^2 - \frac{1}{4} \|\mathbb{E}_{t,k}[\mathbf{d}_{t,k}]\|^2 - \frac{1}{2} \|\nabla f(\mathbf{x}_{t,k})\|^2 + \frac{1}{2} \|\nabla f(\mathbf{x}_{t,k}) - \mathbb{E}_{t,k}[\mathbf{d}_{t,k}]\|^2,
\end{aligned} \tag{15}$$

where the last inequality also follows from the L -smoothness of f . We first have

$$\begin{aligned}
\|\mathbf{y}_{t,k} - \mathbf{x}_{t,k}\|^2 &= \left\| \gamma \left(1 - \frac{\eta}{\tau R}\right) \sum_{i=0}^{k-1} \mathbf{d}_{t,i} - \frac{\eta\gamma\beta}{\tau R(1-\beta)} \mathbf{m}_t \right\|^2 \\
&\leq 2\gamma^2 \left(1 - \frac{\eta}{\tau R}\right)^2 \left\| \sum_{i=0}^{k-1} \mathbf{d}_{t,i} \right\|^2 + \frac{2\eta^2\gamma^2\beta^2}{\tau^2 R^2(1-\beta)^2} \|\mathbf{m}_t\|^2.
\end{aligned} \tag{16}$$

We next bound the second term in (14).

$$\mathbb{E}_{t,k}[\|\mathbf{d}_{t,k}\|^2] = \|\mathbb{E}_{t,k}[\mathbf{d}_{t,k}]\|^2 + \mathbb{E}_{t,k}[\|\mathbf{d}_{t,k} - \mathbb{E}_{t,k}[\mathbf{d}_{t,k}]\|^2] \tag{17}$$

Let $\alpha := \frac{\eta\gamma}{\tau R}$. Combing (14)-(17) leads to that

$$\begin{aligned}
\mathbb{E}_{t,k}[f(\mathbf{y}_{t,k+1}) - f(\mathbf{y}_{t,k})] &\leq -\frac{\alpha}{2} \|\nabla f(\mathbf{x}_{t,k})\|^2 - \frac{\alpha}{2} \left(\frac{1}{2} - \alpha L\right) \|\mathbb{E}_{t,k}[\mathbf{d}_{t,k}]\|^2 + \frac{\alpha^2 L}{2} \mathbb{E}_{t,k}[\|\mathbf{d}_{t,k} - \mathbb{E}_{t,k}[\mathbf{d}_{t,k}]\|^2] \\
&\quad + \frac{\alpha}{2} \|\nabla f(\mathbf{x}_{t,k}) - \mathbb{E}_{t,k}[\mathbf{d}_{t,k}]\|^2 \\
&\quad + 2\alpha\gamma^2 L^2 \left(1 - \frac{\eta}{\tau R}\right)^2 \left\| \sum_{i=0}^{k-1} \mathbf{d}_{t,i} \right\|^2 + \frac{2\alpha^3\beta^2 L^2}{(1-\beta)^2} \|\mathbf{m}_t\|^2.
\end{aligned}$$

Taking the total expectation,

$$\begin{aligned}
\mathbb{E}[f(\mathbf{y}_{t,k+1}) - f(\mathbf{y}_{t,k})] &\leq -\frac{\alpha}{2} \mathbb{E}[\|\nabla f(\mathbf{x}_{t,k})\|^2] - \frac{\alpha}{2} \left(\frac{1}{2} - \alpha L\right) \mathbb{E}[\|\mathbb{E}_{t,k}[\mathbf{d}_{t,k}]\|^2] + \frac{\alpha^2 L}{2} \mathbb{E}[\|\mathbf{d}_{t,k} - \mathbb{E}_{t,k}[\mathbf{d}_{t,k}]\|^2] \\
&\quad + \frac{\alpha}{2} \mathbb{E}[\|\nabla f(\mathbf{x}_{t,k}) - \mathbb{E}_{t,k}[\mathbf{d}_{t,k}]\|^2] \\
&\quad + \underbrace{2\alpha\gamma^2 L^2 \left(1 - \frac{\eta}{\tau R}\right)^2 \mathbb{E}\left[\left\| \sum_{i=0}^{k-1} \mathbf{d}_{t,i} \right\|^2\right]}_{D_{t,k}} + \underbrace{\frac{2\alpha^3\beta^2 L^2}{(1-\beta)^2} \mathbb{E}[\|\mathbf{m}_t\|^2]}_{M_t}.
\end{aligned} \tag{18}$$

We can now sum up (18) to bound progress within in one round of local updates. Next, we try to bound progress across outer iterations. From the definition of $\mathbf{y}_{t,k}$ in (11), we have

$$\mathbf{y}_{t+1,0} - \mathbf{y}_{t,\tau} = \mathbf{x}_{t+1,0} - \mathbf{x}_{t,0} + \frac{\eta\gamma}{\tau R} \mathbf{m}_{t+1} = -\eta\gamma \mathcal{S}_r(\mathbf{m}_{t+1}) + \frac{\eta\gamma}{\tau R} \mathbf{m}_{t+1}.$$

By the L -smoothness of f , we have

$$f(\mathbf{y}_{t+1,0}) - f(\mathbf{y}_{t,\tau}) \leq \langle \nabla f(\mathbf{y}_{t,\tau}), \mathbf{y}_{t+1,0} - \mathbf{y}_{t,\tau} \rangle + \frac{L\eta^2\gamma^2}{2} \left\| \frac{1}{\tau R} \mathbf{m}_{t+1} - \mathcal{S}_r(\mathbf{m}_{t+1}) \right\|^2. \tag{19}$$

Taking conditional expectation $\mathbb{E}_{t,\tau}$ (with randomness from \mathcal{S}_r) on (19), and using (13) and Lemma 1, we reach that

$$\mathbb{E}_{t,\tau}[f(\mathbf{y}_{t+1,0}) - f(\mathbf{y}_{t,\tau})] \leq \frac{dL\eta^2\gamma^2}{2}. \quad (20)$$

Using (20), we are now prepared to bound the progress across outer iterations. Taking the total expectation and summing (18) and (20) from $k = 0$ to $k = \tau - 1$ and from $t = 0$ to $t = T - 1$, we obtain:

$$\begin{aligned} \frac{\mathbb{E}[f(\mathbf{y}_{T,0}) - f(\mathbf{y}_{0,0})]}{\tau T} &\leq -\frac{\alpha}{2\tau T} \sum_{t=0}^{T-1} \sum_{k=0}^{\tau-1} \mathbb{E} \|\nabla f(\mathbf{x}_{t,k})\|^2 - \frac{\alpha}{2\tau T} \left(\frac{1}{2} - \alpha L\right) \sum_{t=0}^{T-1} \sum_{k=0}^{\tau-1} \mathbb{E} [\|\mathbb{E}_{t,k}[\mathbf{d}_{t,k}]\|^2] \\ &\quad + \frac{1}{2} \alpha^2 \zeta^2 L + \frac{dL\eta^2\gamma^2}{2\tau} + \frac{\alpha}{2\tau T} \sum_{t=0}^{T-1} \sum_{k=0}^{\tau-1} \mathbb{E} [\|\nabla f(\mathbf{x}_{t,k}) - \mathbb{E}[\mathbf{d}_{t,k}]\|^2] \\ &\quad + \frac{1}{\tau T} \sum_{t=0}^{T-1} \sum_{k=0}^{\tau-1} D_{t,k} + \frac{1}{T} \sum_{t=0}^{T-1} M_t. \end{aligned} \quad (21)$$

B.1.4 Bounding $D_{t,k}$

First, we have

$$\left\| \sum_{i=0}^{k-1} \mathbf{d}_{t,i} \right\|^2 \leq 2 \left\| \sum_{i=0}^{k-1} (\mathbf{d}_{t,i} - \mathbb{E}_{t,i}[\mathbf{d}_{t,i}]) \right\|^2 + 2k \sum_{i=0}^{k-1} \|\mathbb{E}_{t,i}[\mathbf{d}_{t,i}]\|^2.$$

Then, taking total expectation and summing over $k = 0, \dots, \tau - 1$, from the above relation we have

$$\begin{aligned} \sum_{k=0}^{\tau-1} \mathbb{E} \left[\left\| \sum_{i=0}^{k-1} \mathbf{d}_{t,i} \right\|^2 \right] &\leq 2 \sum_{k=0}^{\tau-1} \mathbb{E} \left[\left\| \sum_{i=0}^{k-1} (\mathbf{d}_{t,i} - \mathbb{E}_{t,i}[\mathbf{d}_{t,i}]) \right\|^2 \right] + 2 \sum_{k=0}^{\tau-1} k \sum_{i=0}^{k-1} \mathbb{E} [\|\mathbb{E}_{t,i}[\mathbf{d}_{t,i}]\|^2] \\ &= 2 \sum_{k=0}^{\tau-1} \sum_{i=0}^{k-1} \mathbb{E} [\|\mathbf{d}_{t,i} - \mathbb{E}_{t,i}[\mathbf{d}_{t,i}]\|^2] + 2 \sum_{k=0}^{\tau-1} k \sum_{i=0}^{k-1} \mathbb{E} [\|\mathbb{E}_{t,i}[\mathbf{d}_{t,i}]\|^2] \\ &\leq 2 \sum_{k=0}^{\tau-1} k \zeta^2 + \tau(\tau - 1) \sum_{i=0}^{k-1} \mathbb{E} [\|\mathbb{E}_{t,i}[\mathbf{d}_{t,i}]\|^2] \\ &\leq \tau(\tau - 1) \zeta^2 + \tau(\tau - 1) \sum_{i=0}^{k-1} \mathbb{E} [\|\mathbb{E}_{t,i}[\mathbf{d}_{t,i}]\|^2] \end{aligned} \quad (22)$$

where the first equality follows from the fact that the total expectation of crossing terms of $\|\sum_{i=0}^{k-1} (\mathbf{d}_{t,i} - \mathbb{E}_{t,i}[\mathbf{d}_{t,i}])\|^2$ are zeros due to independence. From (22) we have

$$\frac{1}{\tau T} \sum_{t=0}^{T-1} \sum_{k=0}^{\tau-1} D_{t,k} \leq 2\alpha\tau(\tau - 1)\gamma^2 L^2 \left(1 - \frac{\eta}{\tau R}\right)^2 \left(\frac{\zeta^2}{\tau} + \frac{1}{\tau T} \sum_{t=0}^{T-1} \sum_{k=0}^{\tau-1} \mathbb{E} [\|\mathbb{E}_{t,k}[\mathbf{d}_{t,k}]\|^2]\right). \quad (23)$$

B.1.5 Bounding M_t

By the definition of \mathbf{m}_t and $\mathbf{m}_0 = \mathbf{0}$, we have

$$\begin{aligned} \|\mathbf{m}_t\|^2 &= \left\| \sum_{s=0}^{t-1} \beta^{t-1-s} (1-\beta) \left(\sum_{k=0}^{\tau-1} \mathbf{d}_{s,k} \right) \right\|^2 \\ &\leq 2(1-\beta)^2 \left\| \sum_{s=0}^{t-1} \beta^{t-1-s} \left(\sum_{k=0}^{\tau-1} (\mathbf{d}_{s,k} - \mathbb{E}_{s,k}[\mathbf{d}_{s,k}]) \right) \right\|^2 + 2(1-\beta)^2 \left\| \sum_{s=0}^{t-1} \beta^{t-1-s} \left(\sum_{k=0}^{\tau-1} \mathbb{E}_{s,k}[\mathbf{d}_{s,k}] \right) \right\|^2. \end{aligned} \quad (24)$$

We estimate the right two terms one by one. Taking total expectation and using the same arguments in equality of (22),

$$\begin{aligned} &\mathbb{E} \left[\left\| \sum_{s=0}^{t-1} \beta^{t-1-s} \left(\sum_{k=0}^{\tau-1} (\mathbf{d}_{s,k} - \mathbb{E}_{s,k}[\mathbf{d}_{s,k}]) \right) \right\|^2 \right] \\ &= \sum_{s=0}^{t-1} \beta^{2(t-1-s)} \mathbb{E} \left[\left\| \sum_{k=0}^{\tau-1} (\mathbf{d}_{s,k} - \mathbb{E}_{s,k}[\mathbf{d}_{s,k}]) \right\|^2 \right] \\ &= \sum_{s=0}^{t-1} \beta^{2(t-1-s)} \sum_{k=0}^{\tau-1} \mathbb{E} [\|\mathbf{d}_{s,k} - \mathbb{E}_{s,k}[\mathbf{d}_{s,k}]\|^2] \\ &\leq \tau \zeta^2 \sum_{s=0}^{t-1} \beta^{2(t-1-s)} \leq \frac{\tau \zeta^2}{1-\beta^2}. \end{aligned} \quad (25)$$

Similarly, using Jensen's inequality, we have

$$\begin{aligned} &\mathbb{E} \left[\left\| \sum_{s=0}^{t-1} \beta^{t-1-s} \left(\sum_{k=0}^{\tau-1} \mathbb{E}_{s,k}[\mathbf{d}_{s,k}] \right) \right\|^2 \right] \\ &\leq \tau \left(\sum_{s=0}^{t-1} \beta^{t-1-s} \right) \sum_{s=0}^{t-1} \beta^{t-1-s} \sum_{k=0}^{\tau-1} \mathbb{E} [\|\mathbb{E}_{s,k} \mathbf{d}_{s,k}\|^2] \\ &\leq \frac{\tau}{1-\beta} \sum_{s=0}^{t-1} \beta^{t-1-s} \sum_{k=0}^{\tau-1} \mathbb{E} [\|\mathbb{E}_{s,k} \mathbf{d}_{s,k}\|^2]. \end{aligned} \quad (26)$$

Combing (24)-(26) gives that

$$\begin{aligned} \frac{1}{T} \sum_{t=0}^{T-1} M_t &\leq \frac{4\tau\alpha^3\beta^2\zeta^2L^2}{1-\beta^2} + \frac{4\tau\alpha^3\beta^2L^2}{1-\beta} \frac{1}{T} \sum_{t=0}^{T-1} \sum_{s=0}^{t-1} \beta^{t-1-s} \sum_{k=0}^{\tau-1} \mathbb{E} [\|\mathbb{E}_{s,k}[\mathbf{d}_{s,k}]\|^2] \\ &= \frac{4\tau\alpha^3\beta^2\zeta^2L^2}{1-\beta^2} + \frac{4\tau\alpha^3\beta^2L^2}{1-\beta} \frac{1}{T} \sum_{t=0}^{T-2} \left(\sum_{s=0}^{T-2-t} \beta^s \right) \left(\sum_{k=0}^{\tau-1} \mathbb{E} [\|\mathbb{E}_{t,k}[\mathbf{d}_{t,k}]\|^2] \right) \\ &\leq \frac{4\tau\alpha^3\beta^2\zeta^2L^2}{1-\beta^2} + \frac{4\tau\alpha^3\beta^2L^2}{(1-\beta)^2} \frac{1}{T} \sum_{t=0}^{T-1} \sum_{k=0}^{\tau-1} \mathbb{E} [\|\mathbb{E}_{t,k}[\mathbf{d}_{t,k}]\|^2]. \end{aligned} \quad (27)$$

B.1.6 Convergence rate

Putting (23) and (27) back into (21), we obtain that

$$\begin{aligned}
\frac{\mathbb{E}[f(\mathbf{y}_{T,0}) - f(\mathbf{y}_{0,0})]}{\tau T} &\leq -\frac{\alpha}{2\tau T} \sum_{t=0}^{T-1} \sum_{k=0}^{\tau-1} \mathbb{E} \|\nabla f(\mathbf{x}_{t,k})\|^2 - \frac{\alpha}{2\tau T} \left(\frac{1}{2} - \alpha L\right) \sum_{t=0}^{T-1} \sum_{k=0}^{\tau-1} \mathbb{E} [\|\mathbb{E}_{t,k}[\mathbf{d}_{t,k}]\|^2] \\
&\quad + \frac{1}{2} \alpha^2 \zeta^2 L + \frac{dL\eta^2\gamma^2}{2\tau} + \frac{\alpha}{2\tau T} \sum_{t=0}^{T-1} \sum_{k=0}^{\tau-1} \mathbb{E} [\|\nabla f(\mathbf{x}_{t,k}) - \mathbb{E}[\mathbf{d}_{t,k}]\|^2] \\
&\quad + 2\alpha\tau(\tau-1)\gamma^2 L^2 \left(1 - \frac{\eta}{\tau R}\right)^2 \left(\frac{\zeta^2}{\tau} + \frac{1}{\tau T} \sum_{t=0}^{T-1} \sum_{k=0}^{\tau-1} \mathbb{E} [\|\mathbb{E}_{t,k}[\mathbf{d}_{t,k}]\|^2]\right) \\
&\quad + \frac{4\tau\alpha^3\beta^2\zeta^2 L^2}{1-\beta^2} + \frac{4\tau\alpha^3\beta^2 L^2}{(1-\beta)^2} \frac{1}{T} \sum_{t=0}^{T-1} \sum_{k=0}^{\tau-1} \mathbb{E} [\|\mathbb{E}_{t,k}[\mathbf{d}_{t,k}]\|^2] \\
&\leq -\frac{\alpha}{2\tau T} \sum_{t=0}^{T-1} \sum_{k=0}^{\tau-1} \mathbb{E} \|\nabla f(\mathbf{x}_{t,k})\|^2 - \frac{\alpha C_1}{\tau T} \sum_{t=0}^{T-1} \sum_{k=0}^{\tau-1} \mathbb{E} [\|\mathbb{E}_{t,k}[\mathbf{d}_{t,k}]\|^2] \\
&\quad + \frac{\alpha}{2\tau T} \sum_{t=0}^{T-1} \sum_{k=0}^{\tau-1} \mathbb{E} [\|\nabla f(\mathbf{x}_{t,k}) - \mathbb{E}[\mathbf{d}_{t,k}]\|^2] + C_2,
\end{aligned} \tag{28}$$

where

$$\begin{aligned}
C_1 &= \frac{1}{4} - \frac{1}{2} \alpha L - 2\tau(\tau-1)\gamma^2 L^2 \left(1 - \frac{\eta}{\tau R}\right)^2 - \frac{4\tau^2 \alpha^2 \beta^2 L^2}{(1-\beta)^2}, \\
C_2 &= \alpha^2 \zeta^2 \left[\frac{L}{2} + 2\alpha(\tau-1)L^2 \left(\frac{\tau R}{\eta} - 1\right)^2 + \frac{4\tau\alpha\beta^2 L^2}{1-\beta^2}\right] + \frac{dL\eta^2\gamma^2}{2\tau}.
\end{aligned}$$

When we take parameters to ensure that $C_1 \geq 0$, from (28), we have

$$\frac{1}{\tau T} \sum_{t=0}^{T-1} \sum_{k=0}^{\tau-1} \mathbb{E} \|\nabla f(\mathbf{x}_{t,k})\|^2 \leq \frac{2\mathbb{E}[f(\mathbf{y}_{0,0}) - f(\mathbf{y}_{T,0})]}{\alpha\tau T} + \frac{1}{\tau T} \sum_{t=0}^{T-1} \sum_{k=0}^{\tau-1} \mathbb{E} [\|\nabla f(\mathbf{x}_{t,k}) - \mathbb{E}[\mathbf{d}_{t,k}]\|^2] + \frac{2C_2}{\alpha}. \tag{29}$$

Note that $\mathbf{y}_{0,0} = \mathbf{x}_{0,0}$ since $\mathbf{m}_0 = \mathbf{0}$, and we denote $f_* = \inf_{\mathbf{x} \in \mathbb{R}^d} f(\mathbf{x})$. By taking $\alpha = \sqrt{\frac{n}{\tau T}}$ and recalling that $\alpha := \frac{\eta\gamma}{\tau R}$, we obtain that

$$\begin{aligned}
\frac{1}{\tau T} \sum_{t=0}^{T-1} \sum_{k=0}^{\tau-1} \mathbb{E} \|\nabla f(\mathbf{x}_{t,k})\|^2 &\leq \frac{2(f(\mathbf{x}_{0,0}) - f_*)}{\sqrt{n\tau T}} + \frac{1}{\tau T} \sum_{t=0}^{T-1} \sum_{k=0}^{\tau-1} \mathbb{E} [\|\nabla f(\mathbf{x}_{t,k}) - \mathbb{E}[\mathbf{d}_{t,k}]\|^2] \\
&\quad + \zeta^2 L \sqrt{\frac{n}{\tau T}} + \frac{4nL^2\zeta^2}{T} \left[\left(\frac{\tau R}{\eta} - 1\right)^2 + \frac{2\beta^2}{1-\beta^2}\right] + dLR^2 \sqrt{\frac{n\tau}{T}}.
\end{aligned} \tag{30}$$

Now we return to the constraint of C_1 when $\alpha = \sqrt{\frac{n}{\tau T}}$. Using $\alpha = \frac{\eta\gamma}{\tau R}$ in C_1 and rearranging terms gives that

$$\frac{1}{4} - \frac{1}{2} \sqrt{\frac{nL^2}{\tau T}} - \frac{nL^2}{\tau T} \left[2\tau(\tau-1)\left(\frac{\tau R}{\eta} - 1\right)^2 + \frac{4\tau^2\beta^2}{(1-\beta)^2}\right] \geq 0.$$

The above relation reduces to

$$\begin{aligned}
\frac{\tau T}{nL^2} - 2\sqrt{\frac{\tau T}{nL^2}} + 1 &\geq 8\tau(\tau-1)\left(\frac{\tau R}{\eta} - 1\right)^2 + \frac{16\tau^2\beta^2}{(1-\beta)^2} + 1, \\
\sqrt{\frac{\tau T}{nL^2}} &\geq \left[8\tau(\tau-1)\left(\frac{\tau R}{\eta} - 1\right)^2 + \frac{16\tau^2\beta^2}{(1-\beta)^2} + 1\right]^{1/2} + 1.
\end{aligned}$$

Since

$$\left[\left[8\tau(\tau-1) \left(\frac{\tau R}{\eta} - 1 \right)^2 + \frac{16\tau^2\beta^2}{(1-\beta)^2} + 1 \right]^{1/2} + 1 \right]^2 \leq 16\tau(\tau-1) \left(\frac{\tau R}{\eta} - 1 \right)^2 + \frac{32\tau^2\beta^2}{(1-\beta)^2} + 4,$$

it suffices to have

$$T \geq 4nL^2 \left[4(\tau-1) \left(\frac{\tau R}{\eta} - 1 \right)^2 + \frac{8\tau\beta^2}{(1-\beta)^2} + \frac{1}{\tau} \right].$$

B.2 Proof of Theorem 2

Proof. Since $\mathbf{d}_{t,k}^{(i)} = \nabla F_i(\mathbf{x}_{t,k}^{(i)}, \boldsymbol{\xi}_{t,k}^{(i)})$, we have $\mathbb{E}_{t,k}[\mathbf{d}_{t,k}] = \frac{1}{n} \sum_{i=1}^n \nabla f_i(\mathbf{x}_{t,k}^{(i)})$. Then,

$$\|\nabla f(\mathbf{x}_{t,k}) - \mathbb{E}_{t,k}[\mathbf{d}_{t,k}]\|^2 = \left\| \frac{1}{n} \sum_{i=1}^n \nabla f_i(\mathbf{x}_{t,k}) - \frac{1}{n} \sum_{i=1}^n \nabla f_i(\mathbf{x}_{t,k}^{(i)}) \right\|^2 \leq \frac{L^2}{n} \sum_{i=1}^n \|\mathbf{x}_{t,k} - \mathbf{x}_{t,k}^{(i)}\|^2, \quad (31)$$

where in the last inequality we use Jensen's inequality and L -smoothness of f_i 's. The quantity in (31) is a crucial in analyzing local SGD updates (Khaled et al., 2020). Since $\mathbf{x}_{t,0}^{(i)}$ is synchronized for every t , the local steps in Algorithm 1 is equivalent to that in local SGD. We can use the existing bound for deviations of local iterates in Wang et al. (2019) (equation (87)) or Yu et al. (2019) (Lemma 5 with $\beta = 0$) in (31), then the term of effect of base optimizer in Theorem 1 can be bounded as

$$\frac{1}{\tau T} \sum_{t=0}^{T-1} \sum_{k=0}^{\tau-1} \mathbb{E} \left[\|\nabla f(\mathbf{x}_{t,k}) - \mathbb{E}_{t,k}[\mathbf{d}_{t,k}]\|^2 \right] \leq \frac{L^2}{n\tau T} \sum_{t=0}^{T-1} \sum_{k=0}^{\tau-1} \sum_{i=1}^n \mathbb{E} [\|\mathbf{x}_{t,k} - \mathbf{x}_{t,k}^{(i)}\|^2] \leq \frac{2\gamma^2 L^2 (\sigma^2 \tau + 3\delta^2 \tau^2)}{1 - 12\gamma^2 L^2 \tau^2}. \quad (32)$$

When $\gamma L\tau \leq 1/6$, we have $1/(1 - 12\gamma^2 L^2 \tau^2) \leq 3/2$. Combining this bound with (32), and using $\gamma = \frac{R}{\eta} \sqrt{\frac{n\tau}{T}}$, the bound in Theorem 1 reduces to

$$\begin{aligned} \frac{1}{\tau T} \sum_{t=0}^{T-1} \sum_{k=0}^{\tau-1} \mathbb{E} \|\nabla f(\mathbf{x}_{t,k})\|^2 &\leq \frac{2(f(\mathbf{x}_{0,0}) - f_*)}{\sqrt{n\tau T}} + \frac{3n\tau^2 L^2 R^2 (\sigma^2 + 3\tau\delta^2)}{\eta^2 T} \\ &\quad + \sigma^2 L \sqrt{\frac{n}{\tau T}} + \frac{4nL^2\sigma^2}{T} \left[\left(\frac{\tau R}{\eta} - 1 \right)^2 + \frac{2\beta^2}{1-\beta^2} \right] + dLR^2 \sqrt{\frac{n\tau}{T}}. \end{aligned}$$

When $T \geq 36nL^2 R^2 \tau^3 / \eta^2$, we have $\gamma L\tau \leq 1/6$, and thus $\frac{1}{\tau T} \sum_{t=0}^{T-1} \sum_{k=0}^{\tau-1} \mathbb{E} \|\nabla f(\mathbf{x}_{t,k})\|^2 = O(1/\sqrt{\tau T})$. \square

C Additional experiment details

C.1 Implementations

Our implementations¹ build on nanoGPT² and FairScale³, where we use nanoGPT for GPT-2 (Radford et al., 2019) modeling, and FairScale for distributed training modules.

C.2 Additional experiment results

Comparison with local AdamW. In our experiments, we omit comparisons with Local AdamW, which uses AdamW as the base optimizer for local steps and periodically averages parameters across workers. In Figure 7, we compare the performance of Local AdamW with SlowMo and our proposed method under communication

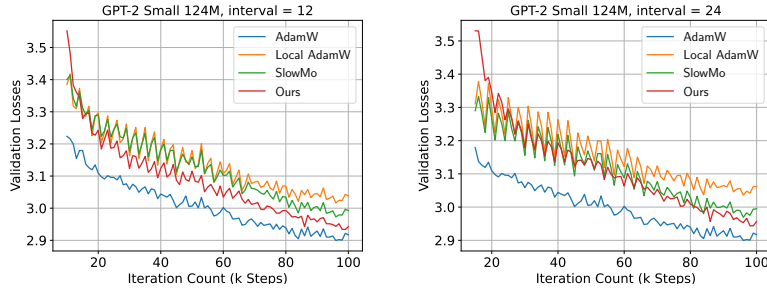


Figure 7: Validation loss curves for communication interval $\tau = 12, 24$.

intervals of $\tau = 12$ and $\tau = 24$. The results show that Local AdamW is significantly slower than both SlowMo and our method, consistent with the findings of Sun et al. (2024).

Comparisons of optimization errors. In addition to the improved generalization performance in terms of validation loss, we evaluate the optimization errors of our proposed method by plotting the training losses in Figure 8 for a communication interval of $\tau = 12$. The results in Figure 8 demonstrate that our method consistently outperforms SlowMo in terms of optimization errors.

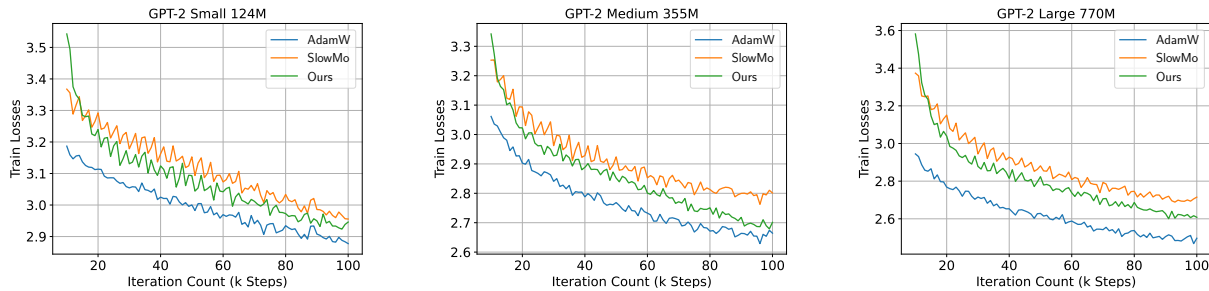


Figure 8: Training loss curves for communication interval $\tau = 12$.

Additional validation loss curves. We plot the validation loss curves in Figures 9 and 10 for communication intervals $\tau = 24$ and $\tau = 36$, respectively. Along with the final validation loss gaps shown in Figure 2, the results indicate improved performance of our proposed sign momentum update compared to the vanilla momentum update in SlowMo.

Details of global AdamW step. In Figure 6, we compare our global sign momentum update with a global update that mimics AdamW, and the corresponding pseudocode is presented in Algorithm 7.

On hyper-parameter fine-tuning. For AdamW, we fine-tune the peak LR and use the recommended values for (β_1, β_2) and weight decay λ from Liu et al. (2024). Our results are consistent with those reported in Liu et al. (2024). The same (β_1, β_2) and λ values are used for the base optimizer AdamW in both SlowMo and our proposed method. For SlowMo, we fine-tune the local peak LR, global LR, and momentum coefficients. In our proposed method, we adopt the values for (β_1, β_2) and λ suggested for Lion in Liu et al. (2024), while fine-tuning only the global LR. Note that our proposed method is more sensitive to communication intervals due to its signed update nature, whereas in SlowMo, the momentum buffer can adapt to the accumulation of gradients from any number of local steps τ , making it less sensitive to communication intervals.

¹<https://github.com/shuhuayu/dist-sign-momentum>

²<https://github.com/karpathy/nanoGPT>

³<https://github.com/facebookresearch/fairscale>

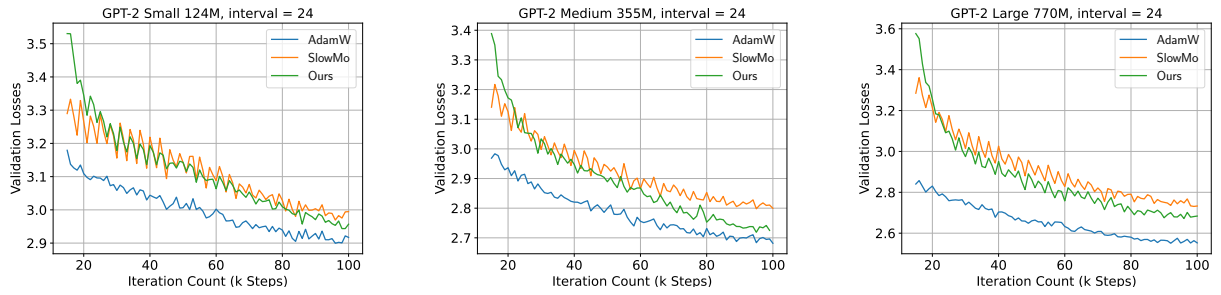


Figure 9: Validation loss curves for communication interval $\tau = 24$.

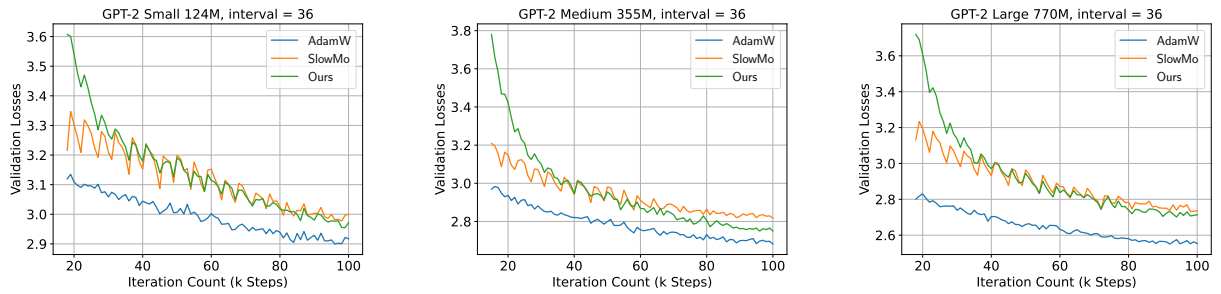


Figure 10: Validation loss curves for communication interval $\tau = 36$.

Algorithm 7 Global AdamW with local steps. Component-wise vector multiplication $\mathbf{g}_t^2 = \mathbf{g}_t \odot \mathbf{g}_t$, and $\sqrt{\widehat{\mathbf{v}}_t}$ means component-wise square root.

Require: Initialization $\mathbf{x}_{0,0}$; local update directions $\mathbf{d}_{t,k}^{(i)}$; local learning rate γ ; global learning rate η ; momentum coefficients β_1, β_2 ; $\epsilon = 10^{-8}$.

```

1:  $\mathbf{m}_t \leftarrow \mathbf{0}, \mathbf{v}_t \leftarrow \mathbf{0}$ 
2: for  $t = 0$  to  $T - 1$  do
3:   for  $i = 1$  to  $n$  in parallel do
4:     for  $k = 0$  to  $\tau - 1$  do
5:        $\mathbf{x}_{t,k+1}^{(i)} \leftarrow \mathbf{x}_{t,k}^{(i)} - \gamma_t \mathbf{d}_{t,k}^{(i)}$ 
6:     end for
7:   end for
8:   All-reduce step:  $\mathbf{x}_{t,\tau} = \frac{1}{n} \sum_{i=1}^n \mathbf{x}_{t,\tau}^{(i)}$ 
9:   Pseudo-gradient:  $\mathbf{g}_t \leftarrow \frac{1}{\gamma_t} (\mathbf{x}_{t,0} - \mathbf{x}_{t,\tau})$ 
10:  Momentum updates:
       $\mathbf{m}_{t+1} \leftarrow \beta_1 \mathbf{m}_t + (1 - \beta_1) \mathbf{g}_t$ 
       $\mathbf{v}_{t+1} \leftarrow \beta_2 \mathbf{v}_t + (1 - \beta_2) \mathbf{g}_t^2$ 
11:  Bias-corrections:
       $\widehat{\mathbf{m}}_{t+1} \leftarrow \mathbf{m}_{t+1} / (1 - \beta_1^{t+1})$ 
       $\widehat{\mathbf{v}}_{t+1} \leftarrow \mathbf{v}_{t+1} / (1 - \beta_2^{t+1})$ 
12:  Parameter update:
       $\mathbf{x}_{t+1,0} \leftarrow \mathbf{x}_{t,0} - \eta \left( \frac{\widehat{\mathbf{m}}_{t+1}}{\sqrt{\widehat{\mathbf{v}}_{t+1} + \epsilon}} + \lambda \mathbf{x}_{t,0} \right)$ 
13:  Synchronize over all workers:
       $\forall i \in [n], \mathbf{x}_{t+1,0}^{(i)} \leftarrow \mathbf{x}_{t+1,0}$ 
14: end for
15: return  $\mathbf{x}_{T,0}$ 

```
